Human Cathepsin V Functional Expression, Tissue Distribution, Electrostatic Surface Potential, Enzymatic Characterization, and Chromosomal Localization‡

Dieter Brömme,*,§ Zhenqiang Li,§ Michel Barnes,⊥ and Ernest Mehler||

Departments of Human Genetics and of Physiology and Biophysics, Mount Sinai School of Medicine, CUNY, New York, NY 10029, and Axys Pharmaceutical, Inc., South San Francisco, CA 94080

Received September 10, 1998; Revised Manuscript Received November 10, 1998

ABSTRACT: Cathepsin V, a thymus and testis-specific human cysteine protease, was expressed in *Pichia pastoris*, and its physicokinetic properties were determined. Recombinant procathepsin V is autocatalytically activated at acidic pH and is effectively inhibited by various cysteine protease class-specific inhibitors. The S2P2 subsite specificity of cathepsin V was found to be intermediate between those of cathepsins S and L. The substrate binding pocket, S2, accepted both aromatic and nonaromatic hydrophobic residues, whereas cathepsins L and S preferred either an aromatic or nonaromatic hydrophobic residue, respectively. In contrast to cathepsin L, but similar to cathepsin S, cathepsin V exhibited only a very weak collagenolytic activity. Furthermore, cathepsin V was determined to be significantly more stable at mildly acidic and neutral pH than cathepsin L, but distinctly less stable than cathepsin S. A homology structure model of cathepsin V revealed completely different electrostatic potentials on the molecular surface when compared with human cathepsin L. The model-based electrostatic potential of human cathepsin V was neutral to weakly positive at and in the vicinity of the active site cleft, whereas that of cathepsin L was negative over extended regions of the surface. Surprisingly, the electrostatic potential of the human cathepsin V model structure resembled that of the model structure of mouse cathepsin L. These differences in the electrostatic potential at the molecular surfaces provide a reactivity determinant that may be the source of differences in substrate selectivity and pH stability. Cathepsin V was mapped to the chromosomal region 9q22.2, a site adjacent to the cathepsin L locus. The high sequence identity and the overlapping chromosomal gene loci suggest that both proteases evolved from an ancestral cathepsin L-like precursor by gene duplication.

Detailed characterization of human cathepsins and the growing number of new members of this papain-like class of proteases have shifted the emphasis of lysosomal cysteine proteases from being nonspecific intracellular house keeping enzymes to proteases exhibiting cell- and tissue-specific functions. This new view is supported by the discovery of an increasing number of tissue-specific proteases. Recently, cathepsin K[1] was identified as a critical cysteine protease (*1*−*5*) involved in bone resorption. In contrast to the ubiquitously expressed cathepsin L, with which cathepsin K shares 64% protein sequence homology (*4*), the latter protease is selectively expressed in osteoclasts and characterized by unique enzymatic properties (*6*). For example, it is the only known cathepsin to cleave type I and II collagens in their triple-helical domains (*6*, *7*). The specific role of cathepsin K in osteoclast-mediated bone resorption has been convincingly demonstrated by the discovery that deficiency in cathepsin K activity causes the bone dysplasia pycnodysostosis (*8*).

Cathepsin W, a further example of a cell-type-specific protease, is exclusively expressed in CD-8$^+$ T-cells (*9*). Although no functional data are presently available, the CTL-specific expression suggests a specific function in T-cell-mediated cytotoxicity.

Cathepsin S, which shares approximately 60−65% amino acid homology with cathepsins L and K, is specifically expressed in lymphatic tissues such as spleen, lymph nodes, and peripheral leukocytes (*10*). Enzyme localization studies revealed a specific expression of cathepsin S in antigen-presenting cells (APC's) such as macrophages, B-cells, and dendritic cells (*9*, *11*, *12*). In vitro experiments demonstrated that cathepsin S is responsible for the specific degradation of the invariant chain of MHC class II complexes, thus suggesting a critical role of the enzyme in antigen presentation (*13*, *14*). Whereas cathepsin S seems to be responsible for the processing of the invariant chain in peripheral APC's, recent findings indicate that cathepsin L is responsible for the degradation of the invariant chain in thymus (*15*−*17*).

‡ In part presented at the AACR Special Conference: Proteases and Protease Inhibitors, Panama City, FL, March 1−5, 1996 and the International Conference on Proteolysis and Protein Turnover, Turku, Finland, September 8−11, 1996.

* To whom correspondence should be addressed: Mount Sinai School of Medicine, Department of Human Genetics, Box 1498, Fifth Avenue at 100th Street, New York, NY 10029. Tel: 212-824-7540. Fax: 212-849-2508. E-mail: brommd01@doc.mssm.edu.

§ Department of Human Genetics, Mount Sinai School of Medicine.

|| Department of Physiology and Biophysics, Mount Sinai School of Medicine.

⊥ Axys Pharmaceutical, Inc.

[1] Abbreviations: SDS, sodium dodecyl sulfate; Z-, benzyloxycarbonyl; -MCA, 4-methyl-7-coumarylamide; E-64, L-3-carboxy-*trans*-2,3-epoxypropionyl-leucylamido-(4-guanidino)butane; Mu-, 4-morpholinecarbonyl; VS, vinyl sulfone; Ph, phenyl; Hph, homophenylalanine. The single letter codes for amino acids were used.

10.1021/bi982175f CCC: $18.00
Published on Web 02/04/1999

Cathepsin L-deficient mice exhibit a defect in MHC class II processing in thymic epithelial cells, which indicates that, for the same proteolytic process, the degradation of the invariant chain, different enzymes have been evolved in different antigen-presenting cells and tissues. It remains unclear, however, how the ubiquitously expressed cathepsin L can fulfill this specific function.

Recently, a novel cathepsin sequence, designated by cathepsin L2 or cathepsin V, was published (*18, 19*). Cathepsin L2 was described as specifically expressed in colon tumor cell lines and in thymus and testis (*19*). Cathepsin V has been described as a major protease in corneal epithelium (*18*). Using degenerate primers designed for highly conserved regions of the active site cysteine and asparagine residues in cathepsins, we have independently identified, cloned, expressed, and characterized the same gene, and originally designated cathepsin U.[2] However, since cathepsins V and L2 represent the same gene, we will use the name cathepsin V. In this paper, we describe the functional expression and enzymatic characterization of this novel protease, its tissue distribution in immune system-related tissues, its differences in the electrostatic potential to cathepsin L, and its chromosomal localization. The thymus-specific expression of cathepsin V and the physicokinetic parameter described in this report suggest that cathepsin V, rather than cathepsin L, may play a critical role in thymic self-antigen presentation and may represent a novel target for the treatment of autoimmune disorders.

EXPERIMENTAL PROCEDURES

Cloning of the Human Cathepsin V cDNA and Construction of an Expression Vector. Degenerate oligonucleotides based on known cDNA sequences of cathepsins K, L, S, and H were designed to regions around the characteristic active site residues for cysteine proteases, C-25 (5′-tgY RgY tSY tgY tgg gcY Wt-3′) and N-175 (5′-cca gSW ggT Ytt SaB BaK cca-3′), and used to amplify cathepsin-specific fragments from a human kidney Quick Clone cDNA (Clontech, Palo Alto, CA). An approximately 450 bp fragment was amplified, cloned into the vector pCR2.1 using the TA cloning system (Invitrogen, San Diego, CA), transformed into TOP10F′ *Escherichia coli* cells, and sequenced on an 373A DNA sequencer (Applied Biosystems, Foster City, CA). One clone was identified to be different from cathepsins L, K, S, H, W, O, and B. To obtain a full-length cDNA, we used a PCR cloning approach. Briefly, cathepsin V-specific primers from the initial PCR product were designed (5′-ggt ggc ttc atg gct agg g-3′ and 5′-tcc agg tgc gac cac tgt g-3′) and used with anchor primers (5′-ggt ggc gac gac tcc tgg-3′ and 5′-ggg cag aca tgg cct gcc c-3′) from a λgt11 human thymus 5′ stretch cDNA library (Clontech, Palo Alto, CA) to clone the missing 5′ and 3′ ends of the full-length cDNA. Two fragments of approximately 600 and 700 bp in length, containing a part of the untranslated 5′ and 3′ ends, were obtained by PCR amplification using *Pfu*-polymerase (Stratagene, LaJolla, CA). The selection of the thymus cDNA library as PCR template was based on northern analyses using the initial PCR product. PCR products were subcloned into the pCR Script SK(+) vector (Stratagene, LaJolla, CA) and sequenced. A full-length cDNA encoding the complete coding region of procathepsin V was obtained by PCR using Quick Clone cDNA from human thymus (Contech, Palo Alto, CA) and the following oligonucleotide primers: 5′-cct tac gta gtt cca aaa ttt gac caa aat ttg gat-3′ and 5′-gct tct aga gct cac aca ttg ggg tag ctg gct gc-3′. Primers contained *Sna*BI and *Xba*I sites for cloning into the *P. pastoris* expression vector pPic9 (Invitrogen, San Diego, CA).

Northern Blot Analysis. A α[^{32}P]-dCTP-labeled 450 bp fragment of cathepsins V was prepared using the Ready-To-Go labeling Kit and Nick columns for purification (Pharmacia, Piscataway, NY). Alternatively, a cathepsin V-specific complement sequence oligonucleotide, 5′-cag agt ggt cgc acc gga a-3′, was labeled with T4 polynucleotide kinase using [^{32}P]-ATP. Multiple tissue northern blots containing mRNAs from various tissues (Clontech, Palo Alto, CA) were prehybridized in Express Hyb solution (Clontech, Palo Alto, CA) and subsequently hybridized with the labeled cathepsin V probe for 1 h at 62 °C. Blots hybridized with the oligonucleotide cathepsin V probe were incubated for 18 h at 55 °C. The blots were washed in 2× SSC/0.05% SDS for 60 min at room temperature and for 60 min at 65 °C in 0.1 x SSC/0.1% SDS (for the 450 bp probes) or at 55 °C for 15 min in 2 × SSPC and 0.2 × SSPC (for the nucleotide probe). As control DNA, a α[^{32}P]-dCTP-labeled GP3DH probe (Clontech, Palo Alto, CA) was used.

Chromosomal Localization of Cathepsin V. Lymphocytes isolated from human blood were cultured in α-MEM medium supplemented with 10% fetal calf serum and phytohemagglutinin (PHA) at 37 °C for 72 h. The lymphocyte cultures were treated with 0.18 mg/mL BrdU (Sigma, St. Louis, MO) to synchronize the cell population. The synchronized cells were washed three times with serum-free medium to release the block and recultured at 37 °C for 6 h in α-MEM with 2.5 μg/mL thymidine (Sigma, St. Louis, MO). Cells were harvested and slides were made by using standard procedures including hypotonic treatment, fix, and air-dry.

A 1 kb cathepsin V probe in pCR-Script Amp SK(+) (Stratagene, LaJolla, CA) was biotinylated with dATP for 1 h at 15 °C using the BRL BioNick labeling kit. The procedure for FISH detection was performed according to Heng at al. (*20*), and slides were denatured in 70% formamide in 2 × SSC for 2 min at 70 °C followed by dehydration with ethanol. Probes were denatured at 75 °C for 5 min in a hybridization mix consisting of 50% formamide and 10% dextran sulfate. Probes were loaded on the denatured chromosomal slides, and after overnight hybridization, slides were washed, detected, and amplified. FISH signals and DAPI banding pattern were recorded separately by taking photographs, and the assignment of the FISH mapping data with chromosomal bands was achieved by superimposing FISH signals with DAPI banded chromosomes (*21*).

Structural Modeling. Structural models of cathepsin V and mouse cathepsin L were built on the basis of the recently published crystallographic structure of human procathepsin L (*22*) determined to a resolution of 2.2 Å. Due to the high sequence identity of both human cathepsin V and mouse cathepsin L to human cathepsin L, the method of homology model building using the MODELLER suite of programs (*23*) was used to obtain the 3-dimensional model structures of cathepsin V and mouse cathepsin L. The resulting structural models were essentially identical to the cathepsin

[2] GenBank accession number: AF070448.

L structure with identical main chain segments having RMS differences of 0.16 and 0.18 Å for cathepsin V and mouse cathepsin L, respectively (it is noted that the coordinates of segments 175−179 of cathepsin L were not reported in the X-ray structure). The molecular graphics were carried out on an SGI platform using the programs INSIGHTII for the CPK representation. The electrostatic potential maps were calculated on the molecular surface with GRASP (*24*) from the crystal structure of cathepsin L and the model structures of cathepsin V and mouse cathepsin L.

Recombinant Cathepsin V: Expression, Activation, and Purification. The PCR construct was ligated into the *Sna*BIII and *Xba*I sites of the pPic-9 expression vector allowing a fusion of the strong secretory yeast α-factor pheromone signal sequence with the procathepsin V sequence. The transfer vector was subsequently linearized with *Bgl*II and electroporated into *P. pastoris* GS115 host cells using standard procedures (Invitrogen, San Diego, CA). His+MutS clones that produced recombinant human cathepsin V were selected and tested for productivity. A *P. pastoris* clone that was expressing high levels of cathepsin V activity was selected for fermentation as described previously (*25*). After centrifugation of the fermentor harvest, the clear supernatant was concentrated (60-fold) using an Amicon Diaflo S1Y10 spiral cartridge to about 100 mL and diafiltered on a YM10 membrane (Amicon) with 50 mM sodium acetate buffer, pH 5.5, containing 2.5 mM EDTA and 2.5 mM dithiothreitol.

The concentrated *P. pastoris* culture supernatant containing recombinant procathepsin V was adjusted to pH 4.0 using 3 M sodium acetate, pH 4.0, and supplemented with dithiothreitol and EDTA (final concentration 0.5 and 2.5 mM, respectively. The activation mixture was incubated in a shaker for 40 min at 37 °C and 200 rpm for autocatalytic processing. The activation was monitored using Z-FR-MCA as a fluorogenic substrate in 100 mM sodium acetate buffer, pH 5.5, containing 2.5 mM EDTA-Na_2 and 2.5 mM dithiothreitol. The activated supernatant was cleared by centrifugation and adjusted to pH 5.5, and ammonium sulfate was added to a final concentration of 1.7 M. After centrifugation at 10000*g*, the cleared supernatant was loaded on a Butyl-Sepharose 4B column (Pharmacia, Piscataway, NY) and washed with 20 mM ammonium acetate, pH 5.0, containing 2 M ammonium sulfate and 0.5 mM dithiothreitol until A_{280} reached baseline. Cathepsin V was eluted from the column using a linear gradient starting with 20 mM ammonium acetate, pH 5.0, containing 2 M ammonium sulfate and 0.5 mM dithiothreitol and ending with 20 mM ammonium acetate, pH 5.0, containing 0.5 mM dithiothreitol. Cathepsin V was the major 280 nm absorbing peak, as determined by activity against the synthetic substrate Z-FR-MCA. The peak fraction eluted at 0.5 M ammonium sulfate. Purified cathepsin V was subjected to N-terminal sequencing.

Recombinant human cathepsin L has been produced in *P. pastoris* (data not shown).

Antibodies of Human Cathepsin V and Western Analyses. A polyclonal antibody (MS19) against the human cathepsin V peptide, GFEGANSNNSK, was raised in New Zealand White rabbits (R. Sargeant, San Ramon, CA). The peptide sequence is part of a surface loop which is structurally conserved in cathepsins K and L and which is characterized by a sequence unique for cathepsin V. The 11-mer peptide was synthesized as a Map-peptide (Dr. Y. Konishi, Biotechnology Research Institute, Montreal, QC). For western analyses, an antibody dilution of 1:5000 was used and signals were detected using POD-labeled anti-rabbit IgG and the ECL substrate (Amersham, Arlington Heights, IL). To determine N-linked glycosylation of recombinant cathepsin V, we incubated unpurified precursor protein from the culture media supernatant for 1 h at pH 5.5 with endoglycosidase F and H (Boehringer, Indianapolis, IN) as recommended by the manufacturer.

Cathepsin V Assays with Methylcoumarylamide Substrates and Type I Collagen. Initial rates of methylcoumarylamide substrate hydrolysis were monitored in 1 cm cuvettes at 25 °C in a Perkin-Elmer fluorimeter at excitation and emission wavelengths of 380 and 450 nm, respectively. The active site concentration of purified cathepsin V was determined by E-64 titration (*26*). Recombinant human cathepsin V was assayed at a constant enzyme concentration (1−10 nM) and variable substrate concentration in 50 mM potassium phosphate buffer, pH 6.5, containing 2.5 mM dithiothreitol and 2.5 mM Na_2EDTA. The kinetic constants, V_{max} and K_m, were obtained by nonlinear regression analysis using the program Enzfitter (*27*).

Soluble calf skin Type I collagen was diluted to 0.4 mg/mL into assay buffers and digested with cathepsin V and L as previously described (*6*). The protease concentration was 50 nM each.

pH Activity Profile and pH Stability. The pH activity profile of human cathepsin V was determined at 1 μM substrate (Z-FR-MCA) concentration ([S] < K_m where the initial rate, v_o, is directly proportional to the k_{cat}/K_m value). The following buffers were used for the pH activity profile: 100 mM sodium citrate (pH 2.8−5.6) and 100 mM sodium phosphate (pH 5.8−8.0). All buffers contained 1 mM EDTA and 0.4 M NaCl to minimize the variation in ionic strength. A three protonation model was used for least-squares regression analysis of the pH activity data (*28*). The data were fitted to the following equation:

$$(k_{cat}/K_m)_{obs} = (k_{cat}/K_m)/([H^+]/K_1 + 1 + K_2/[H^+])$$

and compared with the pH activity profile of human recombinant cathepsin L.

pH-dependent stability of active cathepsins V and L was determined in 100 mM sodium acetate buffer, pH 5.0, and in potassium phosphate buffer, pH 6.5 and 7.0. At appropriate time intervals aliquots of the incubation mixture were withdrawn and the activity was measured using the fluorogenic substrate assay described above.

RESULTS AND DISCUSSION

Human Cathepsin V cDNA and Chromosomal Gene Localization. In an effort to identify novel papain-like cathepsin cDNA sequences, we used degenerate primers derived from regions surrounding the conserved active site residues, cysteine and asparagine, to screen a human kidney Quick Clone cDNA pool. Twenty eight PCR clones were sequenced that contained fragments of approximately 450 bp. Twenty out of the twenty eight contained cathepsin L, one cathepsin H, six cathepsin-unrelated sequences, and one novel cathepsin-like fragment. The unique PCR fragment displayed several motifs typical for papain-like cysteine proteases. Sequence comparison revealed that it was not

Table 1: Protein Sequence Identities of Cathepsin V with the Cathepsins L, K, S, B, H, O, and W[a]

% to hCTSV	hCTSL	hCTSK	hCTSS	hCTSH	hCTSO	hCTSW	hCTSB
full sequence	77.5	50.5	49.5	39.2	31.4	30.8	24.0
mature sequence	79.5	58.6	58.1	46.8	35.5	34.8	30.8

[a] The sequences were analyzed with the program PCGENE using the Myers and Miller's algorithm.

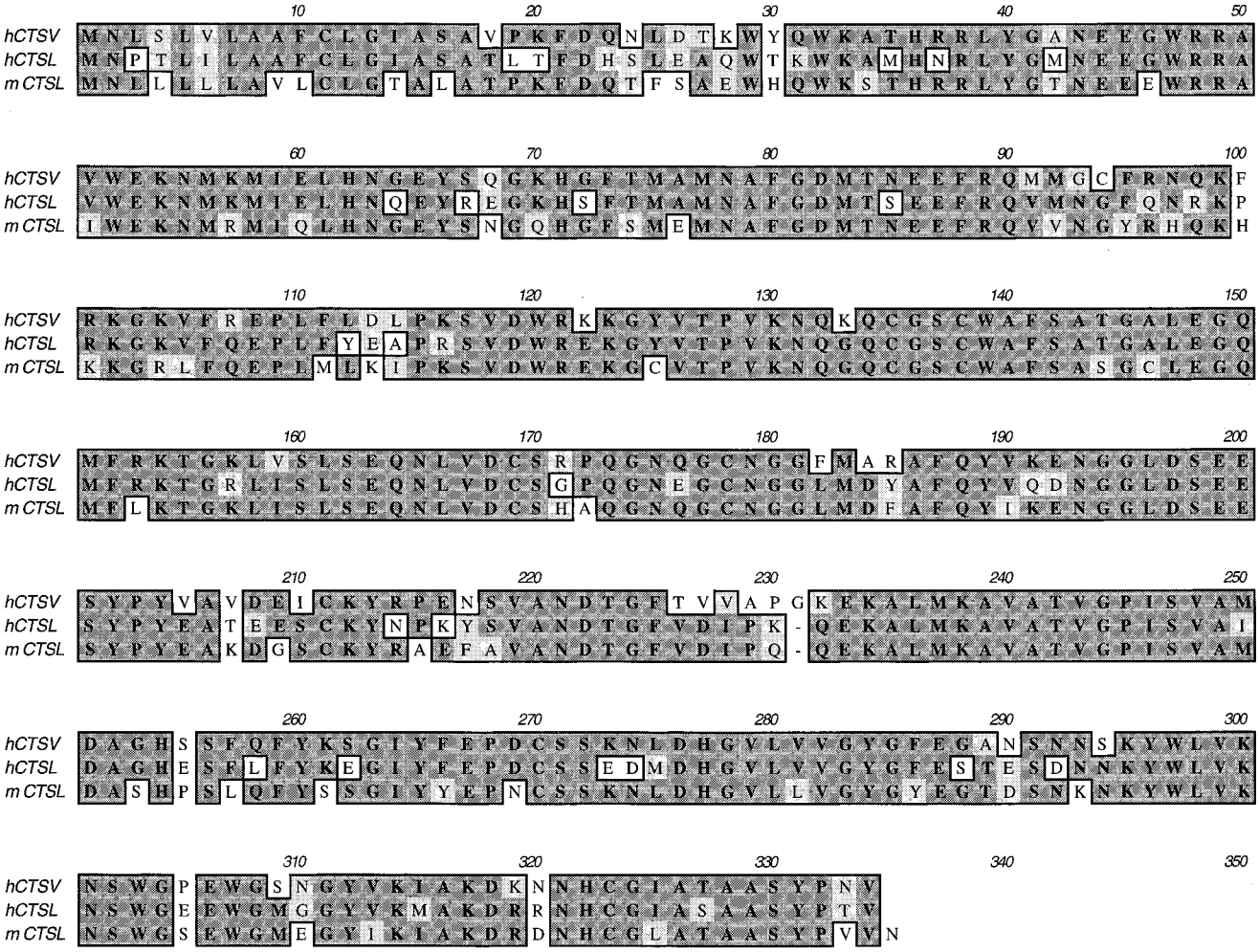

FIGURE 1: Multiple amino acid sequence alignment of human cathepsin V with human cathepsin L and mouse cathepsin L. The amino acid sequences were extracted from the SwissProt database (human cathepsin L precursor, accession P07711; mouse cathepsin L precursor, accession P06797), and the multiple alignment was performed using the Clustal W multiple sequence alignment of MacVector (Oxford Molecular Group, PLC). Identical amino acid residues are dark shaded, similar amino acids are light shaded, and unrelated residue have a white background. Arrowheads mark the putative cleavage sites between the signal sequence and the propart, A_{17}-V_{18}, and between the pro- and the mature regions of the protease (L_{88}-A_{89}). Typical for cathepsins, the second amino acid residue adjacent to the processing site of cathepsin V is a proline.

identical to the sequences of previously identified human cathepsins B, L, H, S, K, C, O, and W. By using specific primers derived from the identified cathepsin-like sequence and anchor primers from a λgt11 cDNA library, we isolated the missing 5′ end including a putative translation initiation start codon (atg) and a 27 bp untranslated region as well as the 3′ end containing the stop codon (tga) and 146 bp of untranslated cDNA. On the basis of the isolated overlapping PCR fragments, the full-length cDNA of human cathepsin V encoded a 334 amino acid protein with a calculated molecular mass of 37329 Da. The open reading frame translated into a putative 17 amino acid signal peptide, a 96 amino acid propeptide, and a 221 amino acid mature region containing the conserved putative active site residues, C-138, H-277, and N-301. The nucleotide sequence encoding the open reading frame of cathepsin V is identical to a sequence referred to as cathepsin V (GenBank accession number: AB001928) and with the exception of two nucleotide exchanges causing an amino acid exchange of residue 81 (Gly → Pro) identical to cathepsin L2 (*19*).

The protein sequence of cathepsin V is highly homologous to human cathepsin L and shares 79.5% identity and 85% homology for the mature proteins and 77.5% identity and 82.9% homology for the preprocathepsins (Table 1 and Figure 1). Homologies are lower for other cathepsins ranging from 62.4% for cathepsin K to 35.1% for cathepsin B (Table 1). Interestingly, a comparison of the human preprocathepsins V and L with mouse preprocathepsin L revealed that human cathepsin V is more closely related to mouse cathepsin L (74.6% identity and 83% homology) than human cathepsin L (71.5% identity and 80.8% homology; Figure 1). As noted above, human cathepsins V and L have sequence identities

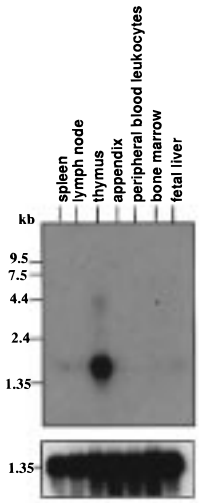

FIGURE 2: Northern blot analysis of human cathepsin V multiple human immune tissue nitrocellulose blot was hybridized with a ^{32}P-labeled human cathepsin V-specific 450bp cDNA probe and with the Clontech GP3DH control probe.

of 77.5%; for example, the divergence of human cathepsins V and L is somewhat smaller than the divergence of the human enzymes to mouse cathepsin L. All other human cathepsins have sequence identities to each other which are smaller than the average identity between orthologues of mouse and human cathepsins (70−80%). This raises the question whether mice possess a cathepsin V orthologue. On the basis of this sequence comparison it is likely that cathepsin V evolved after the mammalian divergence time 90 million years ago (*29*). Efforts to find a mouse orthologue of cathepsin V by PCR and by searching the current EST database failed.

Cathepsin V was localized by FISH analysis on chromosome 9q22.2, a site adjacent to cathepsin L (*30*). The sequence identity of almost 80% between cathepsins L and V and the contiguous localization on chromosome 9 suggest that cathepsins V and L evolved more recently by gene duplication from an ancestral cathepsin L−V-like gene.

mRNA Distribution of Cathepsin V. By screening various immune tissue-related organs, we restricted the transcript of human cathepsin V to the thymus (Figure 2). Other immune-related organs such as fetal liver, appendix, lymph nodes, and bone marrow did not reveal detectable levels of cathepsin V expression. Santamaria et al. (*19*) described the selective expression of cathepsin L2 in colon cancer cell lines, testis, and thymus. While our studies confirm the specific expression of cathepsin V in thymus and testis, we could not demonstrate detectable levels of expression in the colorectal adenocarcinoma cell line SW480 (data not shown). Extended exposure times of the X-ray film to blots hybridized with the 450 bp fragment revealed a cathepsin L-like pattern, indicating a cross-hybridization with cathepsin L mRNA (data not shown). On the contrary, the 5′-labeled cathepsin V-specific probe revealed, also after extended exposure times, only the hybridization signals with the thymus and testis RNA (data not shown).

The specific and high expression level of cathepsin V in thymus suggests a specific function of this novel protease in the regulation of autoimmunity. Recently, it was demonstrated that the related, but ubiquitously expressed, cathepsin L appears to be involved in thymic MHC class II processing during positive selection (*15*). The mechanism by which a non-tissue-specific enzyme, such as cathepsin L, performs

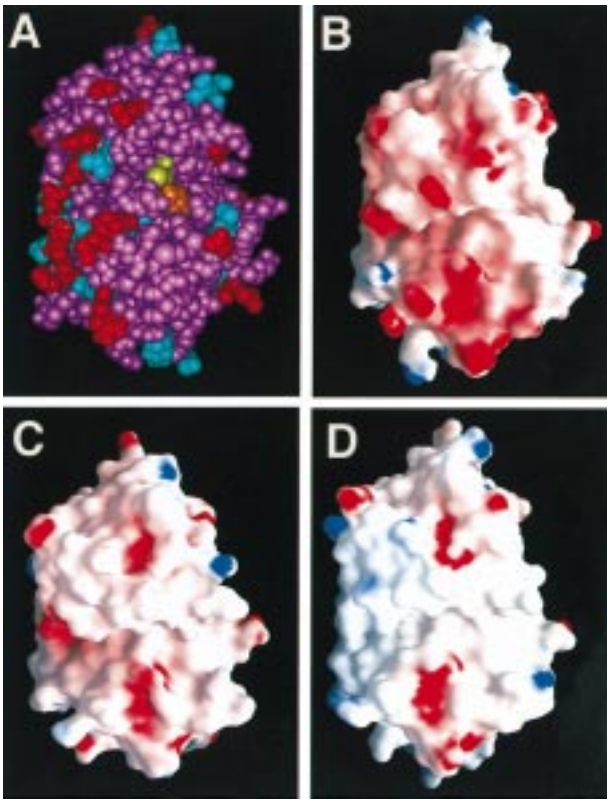

FIGURE 3: Space filling model of human cathepsin L and electrostatic potential maps of human cathepsins L and V and mouse cathepsin L. (A) CPK representation of human cathepsin L (Brookhaven Data Bank, 1CJL) with Cys25 and His163 shown in yellow and orange, respectively. Unchanged residues (cathepsin L and cathepsin V) are in magenta, charge-conserving mutations in cyan, and charge-changing mutations in red. Electrostatic potentials on the molecular surface of human cathepsin L (B), mouse cathepsin L (C), and human cathepsin V (D). The orientation of the molecules in panels B−D are as in A. The color range of the electrostatic potential maps reflects a range from red (−18 kT/mol) via white (neutral) to blue (18 kT/mol).

a thymus-specific function remains unclear. Considering the thymus-specific cathepsin V expression and its high homology to cathepsin L, it is attractive to speculate that in human thymus cathepsin V is involved in the positive T-cell selection. Interestingly, cathepsin V is also highly expressed in the corneal epithelium (*18*).

Electrostatic Potential of the Molecular Surfaces of Human Cathepsins V and L and Mouse Cathepsin L. Although mature human cathepsins V and L share an unusually high protein identity of 77.5%, the calculated isoelectric points of both proteins are strikingly different. The calculated IPs of the complete protein sequence and of the mature cathepsin V are 8.97 and 8.39, respectively, compared to 5.13 and 4.42 for cathepsin L (using PCGENE). For comparison, the calculated IPs for mouse cathepsin L are 6.21 and 4.88, respectively. Out of 69 amino acid exchanges between human procathepsins V and L, 24 increased by one or more units of charge in cathepsin V compared with cathepsin L.

The CPK representation of human cathepsin L in Figure 3A shows the loci of the amino acid changes between cathepsin L and cathepsin V. The view of the structure is oriented so that one looks into the active site with Cys25 (yellow) and His163 (orange) accessible to solvent. The high sequence identity between the two proteinases is clearly apparent in the figure, and it is seen that the Cys25-His163 dyad is surrounded by a relatively large region of identical

residues that probably serves to conserve the local structural and physical characteristics of the active site region. Based on the homology model of cathepsin V and the crystal structure of cathepsin L, Figure 3A also shows that the charge changing mutations are primarily located to the left of the active site, and that their steric adjacencies form several large, surface-exposed patches of altered charge. This region includes the S subsite substrate binding cleft in cathepsins. The upward shift of the calculated isoelectric point in cathepsin V by about 4 pH units is in accordance with the observation that most charge-changing mutations are toward higher basicity.

Comparison of the electrostatic potential map of the human cathepsin L structure (Figure 3B) with that of the human cathepsin V model (Figure 3D) shows that, despite the extensive sequence identity and structural similarity between the crystal structure and model, their electrostatic potentials on the molecular surfaces are remarkably different. The potential of cathepsin L is negative over extended regions of the surface, including the active site cleft. A small more strongly negative patch is seen at the left-hand edge of the cleft. In contrast, the model of cathepsin V shows only a few localized patches of negative potential, and the entire left-hand region of the visible surface tends to be weakly positive. The putative active site cleft of the model is approximately neutral, suggesting that primarily hydrophobic interactions are important for substrate docking, whereas in cathepsin L an electrostatic component is indicated as well. These differences in the electrostatic potential at the molecular surfaces provide a reactivity determinant that may be the source of differences in substrate selectivity of these two cysteine proteinases.

Since an orthologue of cathepsin V has not been found in mouse, but the sequence identity of mouse cathepsin L is closer to that of human cathepsin V than to human cathepsin L (Table 1), it is of interest to compare the electrostatic potential of mouse cathepsin L with both of the human cathepsins. The electrostatic potential map calculated from the model structure of mouse cathepsin L is given in Figure 3C. It is clear that it is intermediate between the electrostatic potentials of human cathepsins L and V and is more negative than cathepsin V, but considerably less negative than human cathepsin L. It is noteworthy that in the model the central portion of the surface, including the active site cleft, shows a very weak potential, similar to that of cathepsin V. At the same time the region of negative potential at the left end of the cleft is not present in cathepsin V, but is clearly seen in human cathepsin L. Thus, the modeling suggests that the active site of mouse cathepsin L may be able to accommodate both types of substrates that are processed differentially in humans by cathepsin L or cathepsin V.

Inspection of the "back" surface of Figure 3A (not shown) showed only two mutations that change charge and four additional charge-conserving changes. Because of this, the differences in the electrostatic potential maps of the back surface of all three proteins are much less (Figure 3B−D). Interestingly then, most of the amino acid changes between cathepsin L and cathepsin V are confined to the face of each protein where the active site is accessible. The loci of the changes are in regions that would most strongly affect selectivity and reactivity and lend further support to the hypothesis that the difference in the electrostatic properties of the two proteins is a determinant of their different substrate selectivity and that mouse cathepsin L may have selectivity that overlaps both human forms.

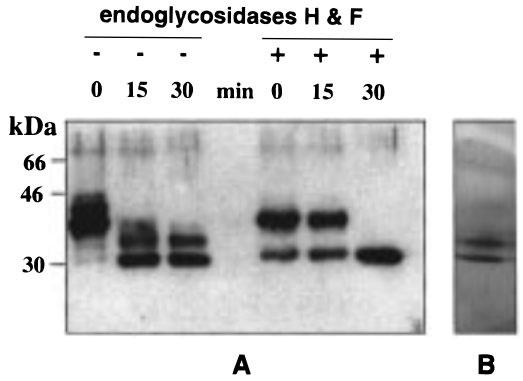

FIGURE 4: Maturation and glycosylation of human cathepsin V. (A) Preparations of crude procathepsin V were incubated in the presence or absence of endoglycosidases H and F for 1 h in 100 mM acetate buffer, pH 5.5. Then, the pH was adjusted to 4.0 and aliquots were loaded on a 10% SDS Tris-Glycine gel after 0, 15, and 30 min incubation times. Proteins were visualized by western blot analysis using the antibody MS19 at a 1:10000 dilution. Treatment with endoglycosidases H and F results in decreased molecular weights of the pro-enzyme by approximately 7 kDa and by 4 kDa for the mature cathepsin V, indicating that both the proregion and the mature part of recombinant cathepsin V are N-linked glycosylated. (B) Silver stained SDS−polyacrylamide gel of purified glycosylated mature cathepsin V. Molecular mass standards (kDa) are indicated in the left margin.

Expression, Activation, and Purification of Recombinant Human Cathepsin V. Human cathepsin V was expressed in *P. pastoris* as a fusion protein containing the α-pheromone signal sequence for extracellular targeting and the procathepsin V open reading frame. The expression level of the protease in the culture supernatant following autoactivation at pH 4.0 was monitored by its Z-FR-MCA hydrolyzing activity inhibitable with 10 μM E-64. The culture supernatant was collected after 3 days of fermentation and concentrated 20-fold by ultrafitration. Activation of the inactive precursor was achieved by autoactivation at pH 4.0. Maximal Z-FR-MCA hydrolyzing activity was achieved after 30 min at 37 °C. Autocatalytic processing of the 38−45 kDa precursor forms resulted in mature forms of approximately 31−35 kDa (Figure 4A).

The deduced amino acid sequence of cathepsin V contained three putative N-glycosylation sites, one located in the signal sequence (N_2-L-S) and two in the mature region (N_{221}-D-T; N_{292}−N-S). Recombinant cathepsin V polypeptides were partially and heterogeneously glycosylated and had molecular masses between 38−45 kDa for the precursor molecule and 31−35 kDa for the mature protease, respectively. After treatment with endoglycosidases H and F, the molecular masses decreased to approximately 38 and 31 kDa, respectively, and migrated as single bands in 10% SDS gels (Figure 4A).

Activated cathepsin V was purified at room temperature on Butyl Sepharose 4B, resulting in two electrophoretically homogeneous and active proteins with apparent molecular masses of 31 and 34 kDa (Figure 4B) that were used for the physicokinetic characterization of the protease. N-terminal sequencing of both bands revealed the same processing site for papain-like cathepsins with a proline adjacent to the N-terminal leucine (NH2-LPKSVDXRKKGY), thus suggesting that both proteins differ only in their degree of glycosylation (Figure 4B).

Table 2: Kinetic Parameters for the Hydrolysis of Peptidyl-MCA Substrates by Recombinant Human Cathepsin V

substrate	k_{cat} (s^{-1})	K_m (μM)	k_{cat}/K_m (M^{-1} s^{-1})
Z-FR-MCA	0.71 ± 0.06	6.4 ± 1.5	110 937 (100%)[a]
Z-LR-MCA	0.41 ± 0.05	4.5 ± 1.4	91 111 (82%)
Z-VR-MCA	0.38 ± 0.01	76 ± 3	5 000 (4.5%)
Z-RR-MCA	0.011 ± 0.001	168 ± 26	65 (0.06%)
Z-LLR-MCA	0.02 ± 0.002	0.7 ± 0.3	28 570
	(8.5 ± 1.1)	0.5 ± 0.1)	(17 000 000) hCTSL
Z-VVR-MCA	0.15 ± 0.01	8.1 ± 0.8	18 520
	(4.1 ± 0.2)	(2 ± 0.2)	(2 050000) hCTSL

[a] Relative activities of the k_{cat}/K_m values referred to the best substrate Z-FR-MCA = 100%. Values in parenthesis for Z-LLR-MCA and Z-VVR-MCA were determined for recombinant human cathepsin L (hCTSL).

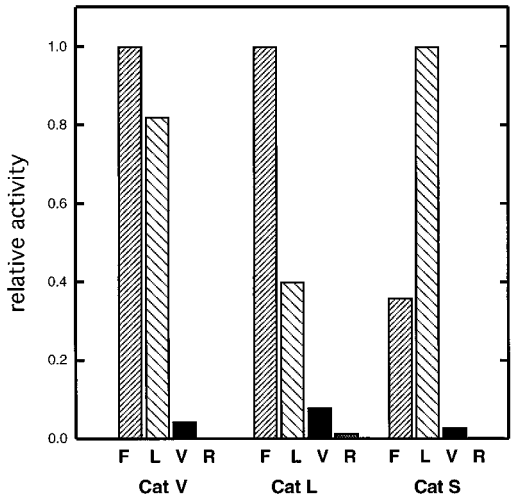

FIGURE 5: k_{cat}/K_m values for the hydrolysis of Z-XR-MCA by cathepsins V, L, and S. Values were normalized to the best substrate = 1. Cathepsin V (Z-FR-MCA, 110 937 M^{-1} s^{-1}); cathepsin L (Z-FR-MCA, 5 111 000 M^{-1} s^{-1}); and cathepsin S (Z-LR-MCA, 243 000 M^{-1} s^{-1}). Data for cathepsins L and S was taken from ref *6*.

Physicokinetic Characterization of Human Cathepsin V. Recombinant mature cathepsin V is a potent hydrolase of standard dipeptide substrates such as Z-FR-MCA. The second-order rate constant (k_{cat}/K_m) is comparable to the rates obtained for cathepsin S, K, and B, but approximately 50× lower than for those reported for cathepsin L (Table 2; see legend to Figure 5). The lower cleavage efficiency of cathepsin V is caused by both a decrease in the k_{cat} and an increase in the K_m values. Since in all papain-like proteinases the so-called S_2 subsite pocket defines the primary substrate specificity, the S_2 subsite specificity of cathepsin V was determined with synthetic substrates of the type Z-X-F-MCA (X: F, L, V, R) and compared with the relative activities of cathepsins L and S. The S_2P_2 specificity of cathepsin V is intermediate between those of cathepsins L and S. A hydrophobic aromatic (phenylalanine) and branched residue (leucine) were equally accepted. This is in contrast to the cathepsins L and S, which prefer either an aromatic or a nonaromatic hydrophobic residue, respectively. All three cathepsins have in common that the β-branched valine and a positively charged arginine residue in P_2 result in poor substrate hydrolysis (Figure 5). These differences may be exploited in the design of future inhibitors of cathepsin V. Differences in the substrate specificity between the closely related cathepsins V and L may be attributed to differences in the geometry of the S_2 binding pocket. In a structure of a papain−inhibitor complex six amino acid residues have been identified to form the S_2 subsite (*31*). On the basis of the homology structure model of cathepsin V, these residues are Phe-182, Met-183, Ala-249, Leu-275, Gly-278, and Ala-328 in cathepsin V (numbering from Figure 1). Whereas the equivalent residues 183, 249, 278, and 328 are identical in cathepsins V and L, the Phe-182 and Leu-275 residues in cathepsin V are replaced by leucine and methionine in cathepsin L. Interestingly, cathepsin S has in these two positions a phenylalanine and a valine residue, respectively. This suggests that the S_2 binding pocket in cathepsin V is a hybrid of the appropriate cathepsin L and S subsites, thereby possibly explaining the cathepsin L- and S-related specificity of cathepsin V.

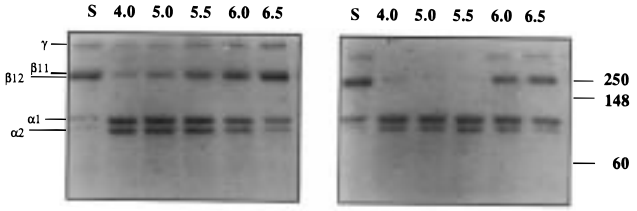

FIGURE 6: SDS−PAGE of type I collagen (soluble calf skin collagen) after digestion with recombinant cathepsins V and L. Digestion of type I collagen at 28 °C and at pH 4.0, 5.0, 5.5, 6.0, and 6.5 in the presence of human cathepsins V (right panel) and L (left panel) (each 50 nM) for 12 h is shown. Before loading on the SDS−PAGE gel, the cathepsins were inactivated with 10 μM E-64. Untreated collagen was used as standard (S). Molecular mass standards are indicated in the right lane.

Santamaria et al. (*19*) described the expression of a cathepsin L2-glutathione S-transferase fusion protein in *E. coli*. The fusion product exhibited a weak Z-FR-MCA activity which was only partially inhibited by E-64. The specific activity of the recombinant protease produced in yeast and described in this report is at least 15000-fold higher, and the protease is completely inhibited at 0.1 μM E-64 concentration. The differences in activity of both preparations are certainly attributable to the different expression systems used. Papain-like cysteine proteases expressed in *E. coli* frequently require extensive refolding procedures that do not always result in active proteins. Adachi et al. reported the expression of recombinant cathepsin V in the baculovirus system and demonstrated the hydrolysis of bovine serum albumin by the protease (*18*).

Unlike cathepsin L, which is known to have significant collagenase activity at acidic pH, the collagenase activity of cathepsin V was found to be very weak. Furthermore, cathepsin L is able to convert the γ and β forms of native type I collagen at pH 4 to 5.5 into the α-forms by cleaving in the telopeptide region, but only a minor decrease of the γ-form in the presence of cathepsin V and at pH 4 and 5 was observed (Figure 6). This shows that, despite their high sequence homologies, both proteases exercise very different substrate specificities.

Recombinant human cathepsin V is strongly inhibited by general cysteine protease inhibitors such as E-64, cystatin, peptidyl vinyl sulfones (*32*), and iodoacetic acid. In addition, various peptide aldehydes such as leupeptin, chymostatin, and calpeptin inhibited cathepsin V at 0.1 μM. Peptide aldehydes are equally potent toward cysteine and serine proteases. As expected, class-specific serine, aspartyl, and metalloprotease inhibitors did not inhibit cathepsin V (Table 3).

Cathepsin L is known to be extremely labile at neutral pH (*33*). Since cathepsins L and V display significant

Table 3: Inhibitor Profile of Human Cathepsin V

	inhibitor	[I]	% inhibition
serine protease inhibitors	PMSF	1 mM	0
	befablock	0.2 mM	0
	DIC	0.1 mM	0
serine/cysteine protease inhibitors	leupeptin	0.1 μM	100
	chymostatin	0.1 μM	100
	calpeptin	0.1 μM	100
metallo-protease inhibitor	EDTA	5 mM	0
aspartyl protease inhibitor	pepstatin	10 μM	0
cysteine protease inhibitors	E-64	0.1 μM	100
	iodoacetic acid	50 μM	95
	chicken cystatin	0.1 μM	100
	Mu-L-hPh-VS-Ph	0.1 μM	100
	Mu-Np-hPh-VS-Np	0.1 μM	100

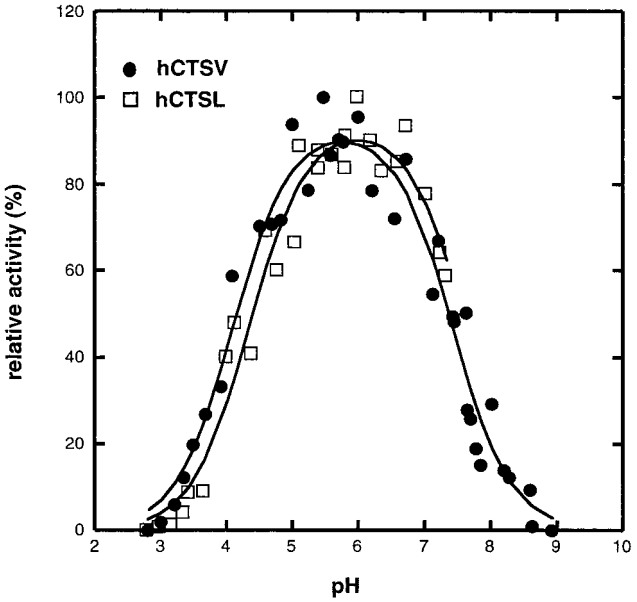

FIGURE 7: pH activity profiles for recombinant human cathepsins V and L. Relative k_{cat}/K_m values for the hydrolysis of Z-FR-MCA by cathepsins V and L were plotted against the pH values. Cathepsin V has a bell-shaped pH activity profile with a pH optimum at pH 5.5 and flanking pK_1 and pK_2 values of 3.9 and 7.4, respectively. In contrast, for cathepsin L, only the ascending limb could be determined due to the instability of the protease at neutral pH.

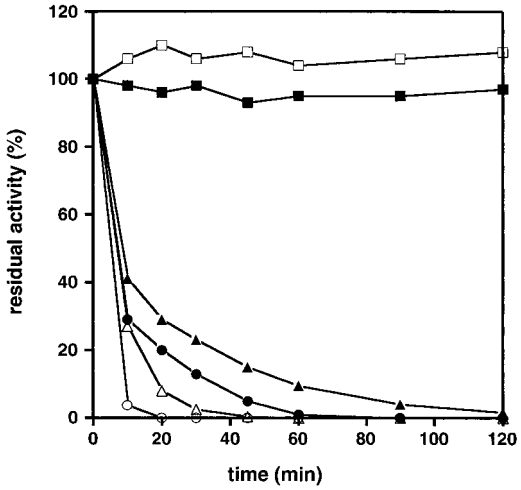

FIGURE 8: pH stability of human cathepsin V and L. Human cathepsins V (filled symbols) and L (open symbols) were incubated in 100 mM acetate buffer, pH 5.5 (rectangles), in 100 mM phosphate buffer, pH 6.5 (triangles), and in 100 mM phosphate buffer, pH 7.0 (circles). All buffers were supplemented with 2.5 mM EDTA and 2.5 mM dithiothreitol. Aliquots of the incubation mixture were withdrawn at the indicated time points, and the residual activities of the cathepsins were measured against 5 μM Z-FR-MCA in 100 mM acetate buffer, pH 5.5, containing 2.5 mM EDTA and 2.5 mM dithiothreitol.

differences in their calculated isoelectric points (see above), the pH-dependent activity profiles and the stability of both proteases were determined and compared. The pH optimum for cathepsin V was 5.7 and close to the value of 5.9 found for recombinant human cathepsin L. However, in contrast to cathepsin L, the pH activity profile of cathepsin V was bell-shaped with flanking pK values of 4.1 and 7.4 (Figure 7). No pK_2 value of human cathepsin L could be determined by reason of its instability at neutral pH. The width of the pH profile (pK_2 − pK_1), which reflects the stability of the ion pair formed by the active site residues cysteine and histidine (*34*), was 3.3 for cathepsin V, a value similar to that of the neutral pH stable cathepsin S (*6*).

To determine differences in the pH stability between cathepsins V and L, we incubated both proteases at pH 5.5, 6.5, and 7.0 at 37 °C and measured the residual activities after appropriate time intervals (Figure 8). Cathepsins V and L were stable at pH 5.5 for 2 h, although they rapidly lost activity at pH 6.5 and 7.0. In contrast, cathepsin V was significantly more stable at these pH values than cathepsin L: thus cathepsin L was completely inactivated after 45 min at pH 6.5 and after 15−20 min at pH 7.0, and cathepsin V still displayed residual activities for 2 h at pH 6.5 and for 1 h at pH 7.0. Considering the thymus-specific expression of cathepsin V and its potential role in MHC class II complex processing, it is interesting that the relative stability of the protease at mildly acidic to neutral pH coincides with the stability of cathepsin S at neutral pH. Cathepsin S has been suggested to be responsible for the invariant chain processing in MHC class II complexes in peripheral antigen-presenting cells. The MHC class II compartment is described as a lysosomal-like compartment (*35*), but recent findings indicate that it may include also mildly acidic to neutral endosomal vesicles (*36*, *37*).

In conclusion, human cathepsin V is a new member of the papain-like protease family that is specifically expressed in the thymus and testis. Protein sequence comparisons revealed that cathepsin V is closely related to human cathepsin L with an amino acid sequence identity for the mature cathepsin as high as 77%. The high sequence identity and the colocalization of cathepsins V and L on chromosome 9 indicate that cathepsin V is probably a recent product of gene duplication from an ancestral cathepsin L−V-like gene.

Despite the high amino acid sequence identity, the electrostatic potentials of the model of cathepsin V and the

structure of cathepsin L in the vicinity of the substrate binding cleft are dramatically different. These differences suggest altered substrate selectivity and other physicokinetic parameters of these two cysteine proteinases. Supporting this hypothesis, the physicokinetic parameters of cathepsin V are clearly distinguished from those of cathepsin L. The preference of cathepsin V to synthetic substrates containing aromatic and nonaromatic hydrophobic P_2 residues, its very weak collagenolytic activity, and its significantly increased pH stability place cathepsin V into a unique class of cysteine proteases intermediate between cathepsins L and S. Similar to cathepsin S, cathepsin V is expressed in antigen-presenting cells (APC) or organs. Cathepsin S is predominantly expressed in peripheral APC's, whereas cathepsin V is specifically expressed in thymus, an organ responsible for T cell selection. The recent finding that mouse cathepsin L is critically involved in the thymic positive selection (*15*), and the fact that human cathepsin V is more closely related to mouse cathepsin L than human cathepsin L, suggest that this novel protease may play a significant role in thymic MHC class II antigen presentation. Localization studies of cathepsin V in human thymus, the processing of the invariant chain by cathepsin V, and its potential role in thymic epithelial cell-mediated antigen presentation are subjects of ongoing experiments.

ACKNOWLEDGMENT

The research has been supported in part by Grants from the National Institue of Health (AR 39191 and AR 41331) and a National Science Foundation Grant (DBI 9732684). We thank Dr. J. Presley (University of California at Davis, Davis, CA) for N-terminal sequencing and Dr. H. H. Q. Heng for performing the FISH analysis (SeeDNA Biotech Inc., North York, ON). Furthermore, we thank Dr. J. Palmer (Axys Pharmaceutical, South San Francisco, CA) for providing two vinyl sulfone inhibitors and Dr. E. Schuchman (Mount Sinai School of Medicine, New York, NY) for the critical reading of the manuscript.

REFERENCES

1. Tezuka, K., Tezuka, Y., Maejima, A., Sato, T., Nemoto, K., Kamioka, H., Hakeda, Y., and Kumegawa, M. (1994) *J. Biol. Chem. 269*, 1106−1109.
2. Inaoka, T., Bilbe, G., Ishibashi, O., Tezuka, K. I., Kumegawa, M., and Kokubo, T. (1995) *Biochem. Biophys. Res. Commun. 206*, 89−96.
3. Shi, G. P., Chapman, H. A., Bhairi, S. M., DeLeeuw, C., Reddy, V. Y., and Weiss, S. J. (1995) *FEBS Lett. 357*, 129−134.
4. Brömme, D., and Okamoto, K. (1995) *Biol. Chem. Hoppe-Seyler 376*, 379−384.
5. Drake, F. H., Dodds, R. A., James, I. E., Connor, J. R., Debouck, C., Richardson, S., Lee-Rykaczewski, E., Coleman, L., Rieman, D., Barthlow, R., Hastings, G., and Gowen, M. (1996) *J. Biol. Chem. 271*, 12511−12516.
6. Brömme, D., Okamoto, K., Wang, B. B., and Biroc, S. (1996) *J. Biol. Chem. 271*, 2126−2132.
7. Kafienah, W., Brömme, D., Buttle, D. J., Croucher, L. J., and Hollander, A. P. (1998) *Biochem. J. 331*, 727−732.
8. Gelb, B. D., Shi, G. P., Chapman, H. A., and Desnick, R. J. (1996) *Science 273*, 1236−1238.
9. Linnevers, C., Smeekens, S. P., and Brömme, D. (1997) *FEBS Lett. 405*, 253−259.
10. Kirschke, H., and Wiederanders, B. (1994) *Methods Enzymol. 244*, 500−511.
11. Chapman, H. A. J., Munger, J. S., and Shi, G. P. (1994) *Am. J. Respir. Crit. Care Med 150*, S155−S159.
12. Reddy, V. Y., Zhang, Q. Y., and Weiss, S. J. (1995) *Proc. Natl. Acad. Sci. U.S.A. 92*, 3849−3853.
13. Riese, R. J., Wolf, P., Brömme, D., Natkin, L. R., Villadangos, J. A., Ploegh, H. L., and Chapman, H. A. (1996) *Immunity 4*, 357−366.
14. Villadangos, J. A., Riese, R. J., Peters, C., Chapman, H. A., and Ploegh, H. L. (1997) *J. Exp. Med. 186*, 549−560.
15. Nakagawa, T., Roth, W., Wong, P., Nelson, A., Farr, A., Deussing, J., Villadangos, J. A., Ploegh, H., Peters, C., and Rudensky, A. Y. (1998) *Science 280*, 450−453.
16. Campbell, P., Nashed, N. Y., Lapinskas, B. A., and Gurrieri, J. (1983) *J. Biol. Chem. 258*, 59−66.
17. Cresswell, P. (1998) *Science 280*, 394−395.
18. Adachi, W., Kawamoto, S., Ohno, I., Nishida, K., Kinoshita, S., Matsubara, K., and Okubo, K. (1998) *Invest. Ophthalmol. Visual Sci. 39*, 1789−1796.
19. Santamaria, I., Velasco, G. M. C., Fueyo, A., Campo, E., and Lopez-Otin, C. (1998) *Cancer Res. 58*, 1624−1630.
20. Heng, H. H. Q., Sqire, J., and Tsui, L.-C. (1992) *Proc. Natl. Acad. Sci. U.S.A. 89*, 9509−9513.
21. Heng, H. H. Q., and Tsui, L.-C. (1993) *Chromosoma 102*, 325−332.
22. Coulombe, R., Grochulski, P., Sivaraman, J., Menard, R., Mort, J. S., and Cygler, M. (1996) *EMBO J. 15*, 5492−5503.
23. Sali, A., and Blundell, T. L. (1993) *J. Mol. Biol. 234*, 779−815.
24. Nicholls, A., Sharp, K. A., and Honig, B. (1991) *Proteins 11*, 281−296.
25. Linnevers, C. J., McGrath, M. E., Armstrong, R., Mistry, F. R., Barnes, M., Klaus, J. L., Palmer, J. T., Katz, B. A., and Brömme, D. (1997) *Protein Sci. 6*, 919−921.
26. Barrett, A. J., Kembhavi, A. A., Brown, M. A., Kirschke, H., Knight, C. G., Tamai, M., and Hanada, K. (1982) *Biochem. J. 201*, 189−198.
27. Leatherbarrow, R. J. (1987) Elsevier Biosoft, Cambridge, U.K.
28. Khouri, H. E., Vernet, T., Menard, R., Parlati, F., Laflamme, P., Tessier, D. C., Gour-Salin, B., Thomas, D. Y., and Storer, A. C. (1991) *Biochemistry 30*, 8929−8936.
29. Wilson, A. C., Carlson, S. S., and White, T. J. (1977) *Annu. Rev. Biochem. 46*, 573−639.
30. Chauhan, S. S., Popescu, N. C., Ray, D., Fleischmann, R., Gottesman, M. M., and Troen, B. R. (1993) *J. Biol. Chem. 268*, 1039−1045.
31. Brocklehurst, K. B., Willenbrook, F. S., and Salih, E. (1987) in *New Comprehensive Biochemistry* (Neuberger, A., and Brocklehurst, K. B., Eds.) pp 39−158, Vol. 16, Elsevier, Amsterdam, New York.
32. Palmer, J. T., Rasnick, D., Klaus, J. L., and Brömme, D. (1995) *J. Med. Chem. 38*, 3193−3196.
33. Turk, B., Dolenc, I., Turk, V., and Bieth, J. G. (1993) *Biochemistry 32*, 375−380.
34. Menard, R., Khouri, H. E., Plouffe, C., Laflamme, P., Dupras, R., Vernet, T., Tessier, D. C., Thomas, D. Y., and Storer, A. C. (1991) *Biochemistry 30*, 5531−5538.
35. Peters, P. J., Neefjes, J. J., Oorschot, V., Ploegh, H. L., and Geuze, H. J. (1991) *Nature 349*, 669−676.
36. Castellino, F., and Germain, R. N. (1995) *Immunity* 2, 73−88.
37. Lutz, M. B., Rovere, P., Kleijmeer, M. J., Rescigno, M., Assmann, C. U., Oorschot, V., Geuze, H. J., Trucy, J., Demandolx, D., Davoust, J., and Ricciardi-Castagnoli, P. (1997) *J. Immunol. 159*, 3707−3716.

BI982175F